DINAME 2017 - Proceedings of the XVII International Symposium on Dynamic Problems of Mechanics
A. T. Fleury, D. A. Rade, P. R. G. Kurka (Editors), ABCM, São Sebastião, SP, Brazil, March 5-10, 2017

Robust Model Predictive Control for Trajectory Tracking by an Unmanned Ground Vehicle - An LMI Approach.

J. L. B. Martins[1], **J. V. Ferreira**[2], **A. R. Fioravanti**[3], **O. Garcia**[4]

[1]joaoluisbm@gmail.com, School of Mechanical Engineering - State Univeristy of Campinas, Brazil.

[2]janito@fem.unicamp.br, School of Mechanical Engineering - State University of Campinas, Brazil.

[3]fioravanti@fem.unicamp.br, School of Mechanical Engineering - State University of Campinas, Brazil.

[4]olmerg@gmail.com , School of Engineering - Jorge Tadeo Lozano University, Colombia.

Abstract: In this paper, a Robust Model Predictive Control (RMPC) strategy is proposed for trajectory tracking by an autonomous vehicle. A bicycle model incremented with a simplified steering system was used to represent the vehicle dynamics. The main objective is to minimize the error between the vehicle's trajectory and the one given by the navigation system. The Small Gain Theorem was used to prove the existence of a stabilizing gain considering mass uncertainty. For solving the optimization problem of the RMPC, this study used Linear Matrix Inequalities (LMIs). The controller developed was validated through simulation in the Matlab *environment for the double lane change maneuver.*

Keywords: Robust Model Predictive Control, Trajectory Tracking, Unmmaned Ground Vehicles, Autonomous Vehicles, LMIs

INTRODUCTION

Unmanned Ground Vehicles (UGV), or Autonomous Vehicles, have been studied for a long time, (Hedrick et al., 1991), (Shladover et al., 1991), (Fritz, 1999). However, a great increase of studies in this area by many research groups and industries took place after the DARPA Grand Challenge in 2005. An automatic driven system is considered the solution for many problems in the cities, as traffic and pollution. Nowadays, autonomous vehicles prototypes are already a reality in the streets and autopilots are incorporated in commercial vehicles. Thus, to turn a vehicle into one fully autonomous, a trajectory tracking system is essential, (Siegwart et al., 2011). It is responsible for keeping the vehicle tracking a desired trajectory, generated by a navigation system, with minimum distance error. This article is part of the project of the autonomous vehicles of the Autonomous Mobility Laboratory (LMA) from the Mechanical Engineering School of Unicamp, which is being developed on a FIAT-PUNTO platform called VILMA (*LMA's Intelligent Vehicle*).

To fulfill the tracking problem, a Model Predictive Control (MPC) strategy is proposed by the present paper. This technique takes into account the system's model and a reference trajectory (Maciejowski, 2002), (Kothare et al., 1996), which makes it suitable for the trajectory tracking problem. There exists many variations of this technique and it has been largely presented in the literature, (Alexis et al., 2016), (Falcone et al., 2010), (Garcia et al., 2013), (Alessandretti et al., 2013). The idea behind the MPC is to use the system's model to make predictions of its future states, compare it with a reference trajectory and, via an optimization problem, compute the optimal input to be applied in the plant in the current time.

As the MPC relies on the system's model, this paper proposed an augmented model, composed by the dynamical vehicle's model and the steering model, (Garcia et al., 2014), (Garcia et al., 2013). Due to the existence of mass uncertainties between the model and the real system, this paper proposes a Robust Model Predictive Control approach, (Kothare et al., 1996). To prove the existence of a robust stabilizing gain, the Small Gain Theorem is applied. To finish, the optimization problem is described through Linear Matrix Inequalities (LMIs). Simulations are made in order to validate the algorithm proposed.

This paper is organized as follows. First, we present the dynamic model of the vehicle and a simplified model of the steering system. The next section introduces the proof for the stabilizing gain followed by an MPC overview. After that, we derive the LMIs used for the optimization problem of the RMPC. To finish, we present the Results and the Conclusion.

VEHICLE MODEL

Vehicle's Dynamics

We are going to use the bicycle model as the vehicle's dynamical model, (Snider, 2009), (Rajamani, 2011) . This model is simple and represents satisfactorily the lateral dynamics of the vehicle. Basically, we consider the vehicle as a rigid body and the two front and rear wheels are lumped into one wheel at the vehicle's centerline, as in Fig. 1:

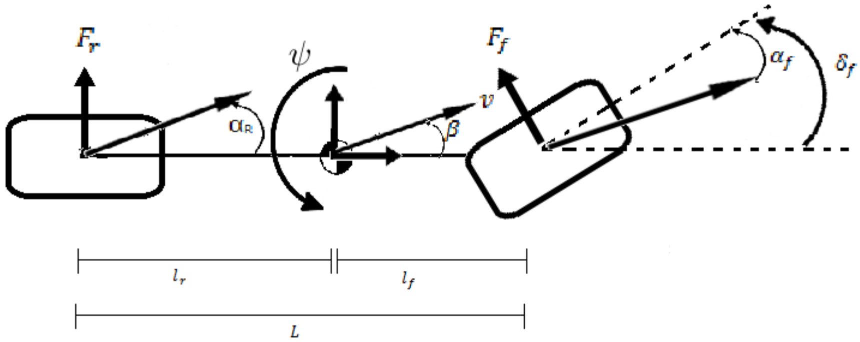

Figure 1 – The Bicycle Model for the vehicle lateral dynamics.

The above subscript f represents the front variables and the r represents the rear ones. In this model, we only consider the front wheel being capable of steering. We are going to consider that the roll and pitch dynamics are negligible and the longitudinal velocity, v_x, is constant. Also, the vehicle is running in a plan surface and the unique external forces acting in the vehicle are the friction forces over the tires. Thus, as in Snider (2009), using Newton and Euler laws, we obtain the following equations for the lateral dynamics:

$$M(\psi v_x + \dot{v}_y) = F_r + F_f \cos \delta_f \tag{1}$$

$$\begin{aligned} J_v \dot{\psi} &= \Sigma T_i \\ &= F_f l_f \cos \delta_f - F_r l_r \end{aligned} \tag{2}$$

in which v_x and v_y are the decomposition of the vehicle's velocity in the local coordinate system, θ is the vehicle's orientation and ψ is its variation, M is the vehicle mass and J_v its inertia. F_f and F_r are the tire's forces and δ_f is the ackermann angle of the front wheels. For the tires friction force, we are going to considerer a proportional model, as in Jazar (2013). Thus, the friction force is proportional to the tire's slip angle, which is given by the difference between the tire direction and the vehicle's velocity direction, represented in Fig. 1 as α_f, for the front tire, and α_r for the rear tire. Hence, for small values of α, the lateral force in the tires is obtained as the slip angle multiplied by the tire's stiffness coefficient:

$$\begin{aligned} F_f &= -2\alpha_f c_f \\ F_r &= -2\alpha_r c_r \end{aligned} \tag{3}$$

As demonstrated in Genta (1997), it is necessary to multiple the equations above by a factor of 2 as each tire in the bicycle model corresponds to the union of two tires. The slip angles, as demonstrated by Jazar (2013), can be obtained decomposing the tire velocity in its lateral and longitudinal components. Therefore, considering small angle approximation, we can obtain:

$$\begin{aligned} \alpha_f &= \frac{v_y + \psi l_f}{v_x} - \delta_f \\ \alpha_r &= \frac{v_y - \psi l_r}{v_x} \end{aligned} \tag{4}$$

Thus, combining Eq. (4), with Eq. (3), Eq. (1) and Eq. (2), and for small angle approximation via Taylor Series, we can obtain the model for the lateral dynamics:

$$\begin{bmatrix} \dot{v}_y \\ \dot{\psi} \end{bmatrix} = \begin{bmatrix} -\frac{v_y}{Mv_x}(2c_f + 2c_r) - \psi(\frac{2c_f l_f - 2c_r l_r}{Mv_x} + v_x) + \frac{2c_f \delta_f}{M} \\ \frac{1}{J_v}[-\frac{v_y}{v_x}(2c_f l_f - 2c_r l_r) - \frac{\psi}{v_x}(2c_f l_f^2 + 2c_r l_r^2) + 2\delta_f c_f l_f] \end{bmatrix} \tag{5}$$

For the trajectory tracking problem, it is more suitable to write the equations with respect to the trajectory, considering the errors of orientation and by the difference between the vehicle center of gravity (CG) and the trajectory, as in the Fig. 2:

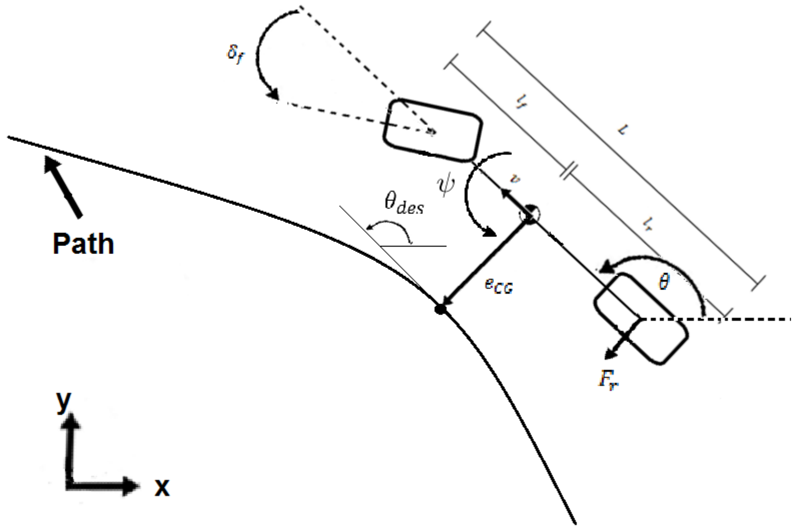

Figure 2 – Bicycle model with respect to the trajectory.

Using the equations described by Garcia et al. (2013), Snider (2009), Genta (1997), we can define the state vector as $\mathbf{x_e} = [e_{cg}\ \dot{e}_{cg}\ \theta_e\ \dot{\theta}_e]^T$, where e_{cg} is the distance between the vehicle CG and the trajectory, θ_{des} is the angle the path makes with the horizontal and θ_e is the orientation error. Therefore, we can derive the lateral dynamics state space as follows:

$$\dot{\mathbf{x}}_\mathbf{e} = \begin{bmatrix} 0 & 1 & 0 & 0 \\ 0 & -\frac{(2c_f+2c_r)}{Mv_x} & \frac{(2c_f+2c_r)}{M} & \frac{-2c_f l_f+2c_r l_r}{Mv_x} \\ 0 & 0 & 0 & 1 \\ 0 & \frac{2c_r l_r-2c_f l_f}{J_v v_x} & \frac{2c_f l_f-2c_r l_r}{J_v} & -\frac{2c_f l_f^2+2c_r l_r^2}{J_v v_x} \end{bmatrix} \mathbf{x_e} + \begin{bmatrix} 0 \\ \frac{2c_f}{M} \\ 0 \\ \frac{2c_f l_f}{J_v} \end{bmatrix} \delta_f + \begin{bmatrix} 0 \\ \frac{2c_r l_r-2c_f l_f}{Mv_x} - v_x \\ 0 \\ -\frac{2c_f l_f^2+2c_r l_r^2}{J_v v_x} \end{bmatrix} \dot{\theta}_{des} + \begin{bmatrix} 0 \\ 0 \\ 0 \\ -1 \end{bmatrix} \ddot{\theta}_{des} \tag{6}$$

Steering System Model

For the steering system, this paper will consider a simplified model. As demonstrated in Garcia et al. (2014), if we ignore the effects of the universal joints and assume that the shafts of the steering system behaves like a rigid body, we can approximate the steering system as seen in Fig. 3:

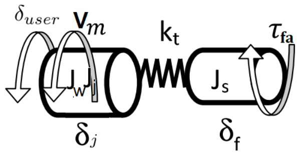

Figure 3 – Simplified steering system model.

in which δ_j is the angle of the joint shaft and the steer shaft and δ_f is the Ackermann angle of the front wheels. Applying the second law of Newton and using as state vector the variables $\mathbf{x_s} = [\delta_j\ \dot{\delta}_j\ \delta_f\ \dot{\delta}_f]^T$, we can obtain the steering state space model:

$$\dot{\mathbf{x}}_\mathbf{s} = \begin{bmatrix} 0 & 1 & 0 & 0 \\ -\frac{k_t}{J_j} & -\frac{C_j+K_e r_g^2 K_i \eta}{J_j} & \frac{k_t r_s}{J_j} & 0 \\ 0 & 0 & 0 & 1 \\ \frac{k_t r_h r_s}{J_s} & 0 & -\frac{k_t r_h r_s^2}{J_s} & -\frac{c_s}{J_w} \end{bmatrix} \mathbf{x_s} + \begin{bmatrix} 0 & 0 & 0 \\ \frac{r_g K_i \eta}{J_s R} & \frac{1}{J_s} & 0 \\ 0 & 0 & 0 \\ 0 & 0 & -\frac{1}{J_w} \end{bmatrix} \begin{bmatrix} V_m \\ \delta_{user} \\ \tau_{fa} \end{bmatrix} \tag{7}$$

in which the inputs $\boldsymbol{u} = [V_m\ \delta_{user}\ \tau_{fa}]^T$ are, respectively, the voltage of the DC motor attached to the steering, which modulate the torque through the static model of the motor, the torque applied by a driver and the torque which depends on the interaction between the tire and the road. Furthermore, J_j, J_s and J_w are the inertias of the steering system, K_e, K_i and R are the voltage and current gains of the motor and its resistance, r_g, η and r_h are mechanic parameters of the steering, defined by Garcia (2016), C_j and c_s are friction coefficients of the steering and k_t is the torsion coefficient of the steering. Using the same logic we used for the tire's forces, we can describe the torque τ_{fa} as:

$$\tau_{fa} = f(\arctan(\frac{-v_y + l_f \psi}{v_x}) - \delta_f) \approx 2c_{mf}(\frac{-v_y + l_f \psi}{v_x} - \delta_f) \tag{8}$$

Notice that this torque depends only on terms that describes the vehicle's dynamical state space ($\boldsymbol{x_e}$), resulting in its elimination as an input of the steering state space, Eq. (7), when both steering and lateral dynamics' state spaces are put together.

Augmented vehicle system

The augmented vehicle system is the combination of the state space of vehicle's dynamics with the state space of the steering system. Considering the following system's dynamics:

$$\begin{aligned} \dot{\mathbf{x}}_{\mathbf{c}} &= \mathbf{A_c x_c} + \mathbf{B_c u_c} \\ \mathbf{y} &= \mathbf{C x_c} \end{aligned} \tag{9}$$

By considering the new state space vector $\mathbf{x_c} = [\mathbf{x_s}\ \mathbf{x_e}]^T$ and the input vector $\mathbf{u_c} = [\theta_{des}\ \dot{\theta}_{des}\ V_m\ \delta_{user}]^T$, the combination results in:

$$\mathbf{A_c} = \begin{bmatrix} 0 & 1 & 0 & 0 & 0 & 0 & 0 & 0 \\ -\frac{k_t}{J_j} & -\frac{C_j + K_e r_g^2 K_i \eta}{J_j} & \frac{k_t r_s}{J_j} & 0 & 0 & 0 & 0 & 0 \\ 0 & 0 & 0 & 1 & 0 & 0 & 0 & 0 \\ \frac{k_t r_h r_s}{J_s} & 0 & -\frac{k_t r_h r_s^2}{J_s} + \frac{2c_{mf}}{J_w} & -\frac{c_s}{J_w} & 0 & \frac{2c_{mf}}{J_w v_x} & -\frac{2c_{mf}}{J_w} & -\frac{2c_{mf} l_f}{J_w v_x} \\ 0 & 0 & 0 & 0 & 0 & 1 & 0 & 0 \\ 0 & 0 & \frac{2c_f}{M} & 0 & 0 & -\frac{(2c_r + 2c_f)}{M v_x} & \frac{(2c_r + 2c_f)}{M} & \frac{2l_r c_r - 2l_f c_f}{M v_x} \\ 0 & 0 & 0 & 0 & 0 & 0 & 0 & 1 \\ 0 & 0 & \frac{2c_f l_f}{J_v} & 0 & 0 & \frac{2l_r c_r - 2l_f c_f}{J_v v_x} & \frac{2l_f c_f - 2l_r c_r}{J_v} & -\frac{2l_r^2 c_r + 2l_f^2 c_f}{J_v v_x} \end{bmatrix} \tag{10}$$

$$\mathbf{B_c} = \begin{bmatrix} 0 & 0 & 0 & 0 \\ \frac{r_g K_i \eta}{J_s R} & \frac{1}{J_s} & 0 & 0 \\ 0 & 0 & 0 & 0 \\ 0 & 0 & -\frac{2c_{mf} l_f}{J_w v_x} & 0 \\ 0 & 0 & 0 & 0 \\ 0 & 0 & \frac{2c_r l_r - 2c_f l_f}{M v_x} - v_x & 0 \\ 0 & 0 & 0 & 0 \\ 0 & 0 & -\frac{2c_r l_r^2 + 2c_f l_f^2}{J_v v_x} & -1 \end{bmatrix}, \mathbf{C} = \begin{bmatrix} 0 & 0 & 0 & 0 & 1 & 0 & 0 & 0 \\ 0 & 0 & 0 & 0 & 0 & 1 & 0 & 0 \\ 0 & 0 & 0 & 0 & 0 & 0 & 1 & 0 \\ 0 & 0 & 0 & 0 & 0 & 0 & 0 & 1 \end{bmatrix} \tag{11}$$

SMALL GAIN THEOREM

Before the design of a robust controller, we must verify if there exist a gain capable of bringing stabilization to the uncertain system. To accomplish this, the present study used the Small Gain Theorem, (Zhou et al., 1996). As a first step, we have to decompose the $\mathbf{A_c}$ matrix isolating the uncertain part, as shown below:

$$\mathbf{A_c} = \mathscr{A} + \mathscr{B}\Delta\mathscr{C} \tag{12}$$

Doing that, we can turn our system into another, composed by the nominal system with the uncertain part acting as the following feedback:

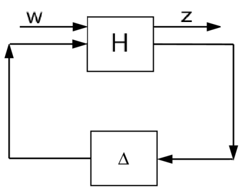

Figure 4 – Block Diagram of the uncertain system.

We are going to consider uncertainties presented in the mass of the vehicle, i.e., $M = M + \delta M$, where δM is unknown. Observe that, in all terms, the mass is located in the denominator, which is very difficult to deal with the uncertainty separation. In order to solve this issue, we can apply an approximation of first order using Taylor's Series, resulting in:

$$\frac{1}{M + \delta M} \approx \frac{1}{M} - \frac{\delta M}{M^2} \tag{13}$$

As a result, we can obtain these matrices for the equation 12:

$$\mathscr{A} = \mathbf{A_c},\ \mathscr{B} = \begin{bmatrix} 0 & 0 \\ 0 & 0 \\ 0 & 0 \\ 0 & 0 \\ 0 & 0 \\ -1 & 0 \\ 0 & 0 \\ 0 & -1 \end{bmatrix}, \Delta = \begin{bmatrix} 0 & 0 & 0 & 0 & 0 & \frac{\delta M}{M^2} & 0 & 0 \\ 0 & 0 & 0 & 0 & 0 & 0 & 0 & \frac{\delta M}{J_v M} \end{bmatrix} \tag{14}$$

$$\mathscr{C} = \begin{bmatrix} 0 & 0 & 0 & 0 & 0 & 0 & 0 & 0 \\ 0 & 0 & 0 & 0 & 0 & 0 & 0 & 0 \\ 0 & 0 & 0 & 0 & 0 & 0 & 0 & 0 \\ 0 & 0 & 0 & 0 & 0 & 0 & 0 & 0 \\ 0 & 0 & 0 & 0 & 0 & 0 & 0 & 0 \\ 0 & 0 & 2c_f & 0 & 0 & -\frac{2c_r+cc_f}{v_x} & 2c_r+2c_f & \frac{2l_r c_r - 2l_f c_f}{v_x} \\ 0 & 0 & 0 & 0 & 0 & 0 & 0 & 0 \\ 0 & 0 & 2c_f l_f & 0 & 0 & \frac{2l_r c_r - 2l_f c_f}{v_x} & 2l_f c_f - 2l_r c_r & -\frac{2l_f^2 c_f + 2l_r^2 c_r}{v_x} \end{bmatrix} \tag{15}$$

Therefore, the system will have a stabilizing gain only if the multiplication of the $\mathscr{H}_\infty$ norm of Δ and the same norm of the system $\mathbf{H}$ is less than or equal to one, i.e.:

$$||\mathbf{H}||_\infty ||\Delta||_\infty \leq 1 \tag{16}$$

MODEL PREDICTIVE CONTROL

The Model Predictive Control technique relies deeply on the system's model. The reason is because the controller uses the model to make future predictions of the system's output state n steps ahead. Considering these predictions, a reference trajectory (the one the system's states should follow) and the past inputs, an optimization problem is derived to found the optimal input to be applied to the plant in the current time. At each new step, the same process is repeated and a new optimization problem is formulated. This type of technique is presented by Camacho and Alba (2013) and Maciejowski (2002). A Block Diagram for the basic structure of the MPC was designed by Camacho and Alba (2013) and evidenced in the Fig. 5:

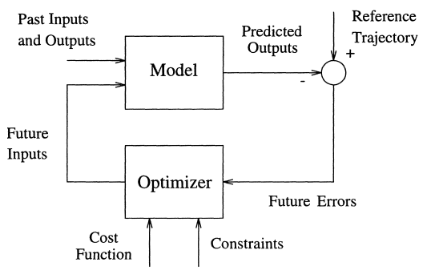

Figure 5 – MPC basic structure.

The Model Predictive Control requires a discrete model of the plant. In our case, as in Garcia (2016), we are going to consider a discretization using the impulse method. Hence, we can derive the following system:

$$\begin{aligned} \mathbf{x_c}[k+1] &= \mathbf{A_d}\mathbf{x_c}[k] + \mathbf{B_d}\mathbf{u}[k] \\ \mathbf{y}[k] &= \mathbf{C_d}\mathbf{x_c}[k] \end{aligned} \tag{17}$$

RMPC - AN LMI APPROACH

The uncertainties of the system can be found in the system's parameters. Assuming, as in Kothare et al. (1996) and Maciejowski (2002), the uncertain system being:

$$\begin{aligned} \mathbf{x}[k+1] &= \mathbf{A}[k]\mathbf{x}[k] + \mathbf{B}[k]\mathbf{u}[k] \\ \mathbf{y}[k] &= \mathbf{C}\mathbf{x}[k] \end{aligned} \tag{18}$$

also assuming the vehicle's mass belongs inside the set $[\delta M_{min}\ \delta M_{max}]Kg$, we can define a polytope as:

$$[\mathbf{A}(\alpha),\mathbf{B}(\alpha)] = \sum_{i=1}^{N} \alpha_i(\mathbf{A}_i,\mathbf{B}_i),\ \alpha_i \geq 0,\ \sum_{i=1}^{N} \alpha_i = 1 \tag{19}$$

Where, as shown in Boyd et al. (1994), for quadratic stability of the polytope, the test in its vertices is enough, thus:

$$\Omega = [\mathbf{A}(0),\mathbf{B}(0)]\ \ [\mathbf{A}(1),\mathbf{B}(1)] \tag{20}$$

For the trajectory tracking problem, as mentioned in Kwakernaak and Sivan (1972), we should consider an augmented system, composed by the system's dynamics and the trajectory's dynamics. Taking the trajectory's dynamics as being:

$$\begin{aligned} \dot{\mathbf{x_r}} &= \mathbf{A_r x_r} \\ \mathbf{z_r} &= \mathbf{C_r x_r} \end{aligned} \tag{21}$$

We can obtain the augmented system through the augmented state $\bar{\mathbf{x}} = [\mathbf{x_c}\ \mathbf{x_r}]^T$. Therefore, one can define the following augmented system:

$$\dot{\tilde{\mathbf{x}}} = \tilde{\mathbf{A}}\tilde{\mathbf{x}} + \tilde{\mathbf{B}}\mathbf{u} \tag{22}$$

Where,

$$\tilde{\mathbf{A}} = \begin{bmatrix} \mathbf{A_c} & \mathbf{0} \\ \mathbf{0} & \mathbf{A_r} \end{bmatrix}, \tilde{\mathbf{B}} = \begin{bmatrix} \mathbf{B} \\ \mathbf{0} \end{bmatrix} \tag{23}$$

This paper proposes to use the cost function for trajectory tracking as defined by Kothare et al. (1996) and shown in Eq. (24):

$$J_\infty[k] = \sum_{i=0}^{\infty} \{ ||\mathbf{Cx}[k+i|k] - \mathbf{C_r x_r}[k+i]||^2_{\mathbf{Q_1}} + ||\mathbf{u}[k+i|k]||^2_{\mathbf{R}} \} \tag{24}$$

in which, $\mathbf{Q_1}$ and $\mathbf{R}$ are weight matrices. Applying this function to the augmented system, Eq. (22), we obtain:

$$J_\infty[k] = \sum_{i=0}^{\infty} \{ ||\tilde{\mathbf{z}}[k+i|k]||^2_{\mathbf{Q_1}} + ||\mathbf{u}[k+i|k]||^2_{\mathbf{R}} \} \tag{25}$$

in which,

$$\tilde{\mathbf{z}}[k] = \tilde{\mathbf{C}}\tilde{\mathbf{x}}[k],\ \tilde{\mathbf{C}} = [\mathbf{C}\ -\mathbf{C_r}] \tag{26}$$

The method used in this paper to make the control robust is given by Kothare et al. (1996) and Maciejowski (2002). Regarding the cost function for trajectory tracking given in Eq. (25), the robustness against uncertainties is obtained by solving the following *min-max* problem:

$$\min_{\mathscr{U}[k]} \max_{\mathbf{A}[k+j],\mathbf{B}[k+j]\in\Omega} J_\infty[k] \tag{27}$$

in which $\mathscr{U}[k]$ is the set of all inputs from $j = 0$ to a determined *Control Horizon* H_u, that is, $\mathscr{U}[k] = [u[k|k]^T, \ldots, u[k+H_u-1|k]^T]^T$ and the maximization is given for all $j > 0$. The notation $[k+i|k]$ represents the $k+i\ th$ input predicted in the current time k. The *min-max* problem is not convex, which invalidates the LMI approach. To get around this, we are going to suppose the existence of a Lyapunov function $V(x) = \boldsymbol{x}^T\mathbf{P}\boldsymbol{x}$, $\mathbf{P} > \mathbf{0}$, and that for all pair of the uncertain system, $\mathbf{x}[k+j|k], \mathbf{u}[k+j|k]$, we have:

$$V(\tilde{\mathbf{x}}[k+j+1|k]) - V(\tilde{\mathbf{x}}[k+j|k]) \leq -||\tilde{\mathbf{z}}||^2_{\mathbf{Q_1}} - ||\mathbf{u}||^2_{\mathbf{R}} = -\tilde{\mathbf{z}}^T\mathbf{Q_1}\tilde{\mathbf{z}} - \mathbf{u}^T\mathbf{R}\mathbf{u} \tag{28}$$

Thus is an upper bound for the Lyapunov function for an *infinite* Control Horizon. Assuming that $J_\infty < \infty$, we have $\boldsymbol{\bar{x}[\infty|k]} = \mathbf{0}$, thus, $V(\bar{\mathbf{x}}[\infty|k]) = 0$. Hence, adding up both sides of Eq. 28 from $j = 0$ to $j = \infty$, we can obtain:

$$-V(\tilde{\mathbf{x}}[k|k]) \leq -J_\infty[k] \tag{29}$$

Once the upper bound equation is assumed to be valid and taking the set of uncertainties of the model $(\mathbf{A_i}, \mathbf{B_i}) \in \Omega$, we have:

$$\max_{[\mathbf{A}(k_j),\mathbf{B}(k+j)]\in\Omega} J_\infty[k] \leq V(\tilde{\mathbf{x}}[k|k]) \tag{30}$$

Hence, we can substitute the *min-max* problem for the optimization problem below:

$$\min_{\mathscr{U}[k]} V(\tilde{\mathbf{x}}[k|k]) \tag{31}$$

Which is the same as solving the following problem:

$$\begin{aligned} &\min_{\gamma,\mathbf{P}} \gamma \\ s.t.: &\ \mathbf{P} > 0 \\ &\tilde{\mathbf{x}}[k|k]^T \mathbf{P} \tilde{\mathbf{x}}[k|k] \leq \gamma \end{aligned} \tag{32}$$

By definition, $\mathbf{P} > \mathbf{0}$, thus, applying a variable substitution $\mathbf{Q} = \gamma \mathbf{P}^{-1} > \mathbf{0}$, and the Schur Complement, we can obtain the first LMI:

$$\begin{bmatrix} \mathbf{Q} & \tilde{\mathbf{x}}[k|k] \\ \tilde{\mathbf{x}}[k|k]^T & 1 \end{bmatrix} \geq 0 \tag{33}$$

Notice that this LMI depends on the system's current state. Taking the upper bound of the Eq. 28, and remembering that the entry is the feedback of the states multiplied by a gain, that is, $\mathbf{u}[k] = \mathbf{K_k}\mathbf{x}[k|k]$, we have:

$$\begin{aligned} V(\tilde{\mathbf{x}}[k+1]) - V(\tilde{\mathbf{x}}[k]) &\leq -\tilde{\mathbf{z}}^T \mathbf{Q_1} \tilde{\mathbf{z}} - \mathbf{u}^T \mathbf{R} \mathbf{u} \\ \tilde{\mathbf{x}}[k+j]^T [(\tilde{\mathbf{A}} + \tilde{\mathbf{B}}\mathbf{K_k})^T \mathbf{P} (\tilde{\mathbf{A}} + \tilde{\mathbf{B}}\mathbf{K_k}) - \mathbf{P} + &\tilde{\mathbf{C}}^T \mathbf{Q_1} \tilde{\mathbf{C}} + \mathbf{K_k}^T \mathbf{R} \mathbf{K_k}] \tilde{\mathbf{x}}[k+j] \leq 0 \end{aligned} \tag{34}$$

In Eq. 34, we have only to analyze the inner expression of the quadratic term. Post and pre multiplying this term by $\mathbf{Q}$, and substituting $\mathbf{P} = \gamma \mathbf{Q}^{-1}$ and $\mathbf{Y} = \mathbf{K}\mathbf{Q}$, we obtain:

$$-(\tilde{\mathbf{A}}\mathbf{Q} + \tilde{\mathbf{B}}\mathbf{Y})^T \mathbf{Q}^{-1} (\tilde{\mathbf{A}}\mathbf{Q} + \tilde{\mathbf{B}}\mathbf{Y}) + \mathbf{Q} - \frac{1}{\gamma} \mathbf{Q} \tilde{\mathbf{C}}^T \mathbf{Q_1} \tilde{\mathbf{C}} \mathbf{Q} - \frac{1}{\gamma} \mathbf{Y}^T \mathbf{R} \mathbf{Y} \geq 0 \tag{35}$$

Hence, applying the Schur Complement, we can find:

$$\begin{bmatrix} \mathbf{Q} & 0 & 0 & (\tilde{\mathbf{A}}\mathbf{Q} + \tilde{\mathbf{B}}\mathbf{Y}) \\ \star & \gamma \mathbf{I_R} & \mathbf{0} & \mathbf{R}^{1/2}\mathbf{Y} \\ \star & \star & \gamma \mathbf{I_{Q_1}} & \mathbf{Q_1}^{1/2} \tilde{\mathbf{C}} \mathbf{Q} \\ \star & \star & \star & \mathbf{Q} \end{bmatrix} \geq \mathbf{0} \tag{36}$$

Which, for each corner of the polytope, must be satisfied. Thus, this, applied in the set $[\mathbf{A}(\mathbf{0}), \mathbf{B}(\mathbf{0})]$ and $[\mathbf{A}(\mathbf{1}), \mathbf{B}(\mathbf{1})]$, form the other two LMIs of the optimization problem. If the optimization problem is feasible, the gain can be retrieved doing $\mathbf{K_k} = \mathbf{Y}\mathbf{Q}^{-1}$.

RESULTS

In our simulations, we are going to consider a mass uncertainty of $\delta M_{min} = 0$ and $\delta M_{max} = 750$. The system was discretized using the impulse method at a sampling time of $10ms$. The parameters values were the same used by Garcia (2016). Thus, applying the norm $\mathscr{H}_\infty$ for the Δ and the $\mathbf{H}$ system, described in Eq. 12, Eq. 14 and Eq. 15, one can obtain:

$$\begin{aligned} &||\mathbf{H}||_\infty = 1.47 \cdot 10^3 \\ &||\Delta||_\infty = 4.22 \cdot 10^{-4} \\ &||\mathbf{H}||_\infty ||\Delta||_\infty = 0.6216 < 1 \end{aligned} \tag{37}$$

Therefore, there exists a robust stable gain capable of stabilizing the system proposed by this paper. For the vehicle simulation, we are going to consider the vehicle performing the double-lane change maneuver, (Forkenbrock et al., 2003), in a flat plane with constant longitudinal velocity of $10m/s$. The trajectory was designed using splines and discretized using the same sampling time of $10ms$. This type of trajectory imposes a great manual skill, which is suitable for autonomous tracking evaluation. We are going to consider the following variables as indicators of performance:

- $|\bar{e}|_{cg}$ and $e_{cg_{max}}$: the mean of the lateral distance and its maximum point.
- $|\bar{\theta_e}|$ and $|\bar{\theta_e}|_{max}$: the mean of the orientation error and its maximum point.

The weight matrices are defined as follows:

$$\mathbf{Q_1} = \begin{bmatrix} 1 & 0 & 0 & 0 \\ 0 & 1 & 0 & 0 \\ 0 & 0 & 1 & 0 \\ 0 & 0 & 0 & 1 \end{bmatrix}, \mathbf{R} = \begin{bmatrix} 1.5 \cdot 10^{-3} & 0 & 0 & 0 \\ 0 & 1.5 \cdot 10^{-3} & 0 & 0 \\ 0 & 0 & 1 & 0 \\ 0 & 0 & 0 & 1 \end{bmatrix} \tag{38}$$

The simulations were performed in the *Matlab* environment using the function *ode45* as integration method. For the LMIs, we used the solver SeDuMi (Sturm, 1999) and the parser YALMIP (Lofberg, 2004). The result of the system without uncertainties and its performance indicators can be seen in Fig. 6 and Tab. 1, respectively.

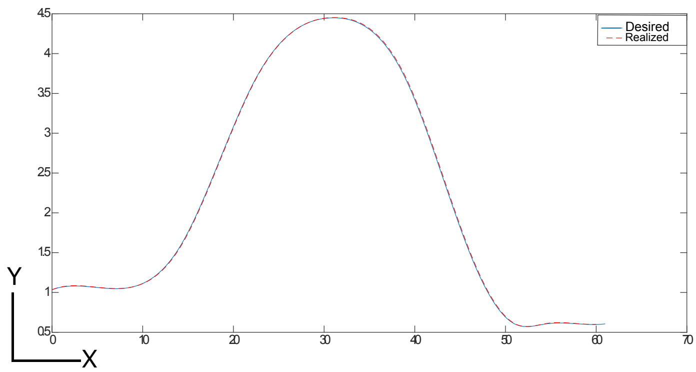

Figure 6 – Trajectory realized with MPC controller without uncertainties.

Table 1 – Performance indicators for MPC controller without uncertainties.

$\lvert e_{cg}\rvert_{max}$ [m]	$\overline{\lvert e_{cg}\rvert}$ [m]	$\lvert\theta_e\rvert_{max}$ [m]	$\overline{\lvert\theta_e\rvert}$ [m]
0.0257	0.0094	0.0606	0.0244

The result of the MPC controller with mass uncertainty of $750Kg$ is shown in Fig. 7 as well as its performance indicators in Tab. 2.

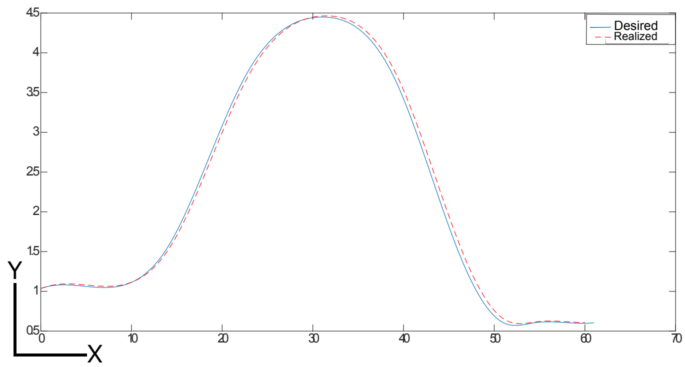

Figure 7 – Trajectory realized by the MPC controller with mass uncertainty of $750kg$.

Table 2 – Performance indicators for MPC controller with mass uncertainty of $750kg$.

$\lvert e_{cg}\rvert_{max}$ [m]	$\overline{\lvert e_{cg}\rvert}$ [m]	$\lvert\theta_e\rvert_{max}$ [m]	$\overline{\lvert\theta_e\rvert}$ [m]
0.1346	0.0482	0.0731	0.03

To conclude, we present the trajectory realized by the car using the RMPC controller for the mass uncertainty problem, its indicators and the main states of the system, in Fig. 8, Tab. 3 and Fig. 9, respectively.

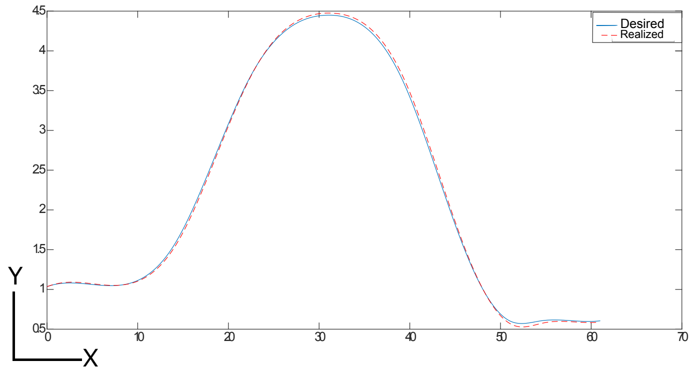

Figure 8 – Trajectory realized by the RMPC controller with mass uncertainty of 750Kg.

Table 3 – Performance indicators for RMPC controller with mass uncertainty of 750Kg.

$\|e_{cg}\|_{max}$ [m]	$\overline{\|e_{cg}\|}$ [m]	$\|\theta_e\|_{max}$ [m]	$\overline{\|\theta_e\|}$ [m]
0.0605	0.0255	0.0651	0.0258

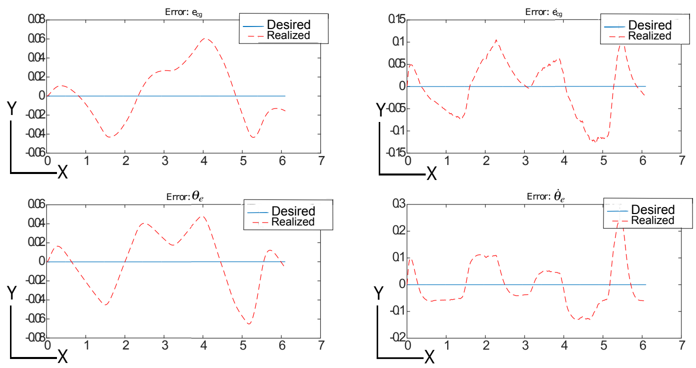

Figure 9 – Trajectory realized by the main states of the system.

As one can see, we have an augment in the errors from the traditional MPC to the one applied in a system containing mass uncertainty. Applying the RMPC, we show that the performance indicators perform better, decreasing the errors by almost half.

CONCLUSION

In this paper, we proposed a Robust Model Predictive Control strategy for trajectory tracking by an autonomous vehicle performing in a flat plane and with constant longitudinal velocity. We presented the results for the system without uncertainty as well as with uncertainties. Also, we demonstrated by simulations that using the RMPC the errors are decreased by half. Future studies should include more variables, as the longitudinal velocity, a banked plane and input saturation. In general, the strategy proposed by this paper showed to be efficient and capable of making the vehicle tracking the desired trajectory.

REFERENCES

Alessandretti, A., Aguiar, A. P., and Jones, C. (2013). Trajectory-tracking and path-following controllers for constrained underactuated vehicles using model predictive control. In *European Control Conference 2013*, number EPFL-CONF-186264.

Alexis, K., Papachristos, C., Siegwart, R., and Tzes, A. (2016). Robust model predictive flight control of unmanned rotorcrafts. *Journal of Intelligent & Robotic Systems*, 81(3-4):443–469.

Boyd, S. P., El Ghaoui, L., Feron, E., and Balakrishnan, V. (1994). *Linear matrix inequalities in system and control theory*, volume 15. SIAM.

Camacho, E. F. and Alba, C. B. (2013). *Model predictive control*. Springer Science & Business Media.

Falcone, P., Borrelli, F., Tseng, E. H., and Hrovat, D. (2010). On low complexity predictive approaches to control of autonomous vehicles. In *Automotive Model Predictive Control*, pages 195–210. Springer.

Forkenbrock, G. J., Garrott, W. R., and Boyd, P. (2003). An overview of nhtsa's recent light vehicle dynamic rollover propensity research and consumer information program. *ESV, Paper*, (488).

Fritz, H. (1999). Longitudinal and lateral control of heavy duty trucks for automated vehicle following in mixed traffic: experimental results from the chauffeur project. In *Control Applications, 1999. Proceedings of the 1999 IEEE International Conference on*, volume 2, pages 1348–1352. IEEE.

Garcia, O. (2016). *Análise de risco para o condicionamento do controle cooperativo de veículos autônomos*. PhD thesis, Unicamp.

Garcia, O., Ferreira, J., and Miranda Neto, A. (2013). Dynamic model of a commercial vehicle for steering control and state estimation. In *In XI Intelligent Atomation Brazilian Symposium (SBAI)*.

Garcia, O., Ferreira, J., and Miranda Neto, A. (2014). Design and simulation for path tracking control of a commercial vehicle using mpc. In *Robotics: SBR-LARS Robotics Symposium and Robocontrol (SBR LARS Robocontrol), 2014 Joint Conference on*, pages 61–66. IEEE.

Genta, G. (1997). *Motor vehicle dynamics: modeling and simulation*, volume 43. World Scientific.

Hedrick, J., McMahon, D., Narendran, V., and Swaroop, D. (1991). Longitudinal vehicle controller design for ivhs systems. In *American Control Conference, 1991*, pages 3107–3112. IEEE.

Jazar, R. N. (2013). *Vehicle dynamics: theory and application*. Springer Science & Business Media.

Kothare, M. V., Balakrishnan, V., and Morari, M. (1996). Robust constrained model predictive control using linear matrix inequalities. *Automatica*, 32(10):1361–1379.

Kwakernaak, H. and Sivan, R. (1972). *Linear optimal control systems*, volume 1. Wiley-interscience New York.

Lofberg, J. (2004). Yalmip: A toolbox for modeling and optimization in matlab. In *Computer Aided Control Systems Design, 2004 IEEE International Symposium on*, pages 284–289. IEEE.

Maciejowski, J. M. (2002). *Predictive control: with constraints*. Pearson education.

Rajamani, R. (2011). *Vehicle dynamics and control*. Springer Science & Business Media.

Shladover, S. E., Desoer, C. A., Hedrick, J. K., Tomizuka, M., Walrand, J., Zhang, W.-B., McMahon, D. H., Peng, H., Sheikholeslam, S., and McKeown, N. (1991). Automated vehicle control developments in the path program. *IEEE Transactions on vehicular technology*, 40(1):114–130.

Siegwart, R., Nourbakhsh, I. R., and Scaramuzza, D. (2011). *Introduction to autonomous mobile robots*. MIT press.

Snider, J. M. (2009). Automatic steering methods for autonomous automobile path tracking. *Robotics Institute, Pittsburgh, PA, Tech. Rep. CMU-RITR-09-08*.

Sturm, J. F. (1999). Using sedumi 1.02, a matlab toolbox for optimization over symmetric cones. *Optimization methods and software*, 11(1-4):625–653.

Zhou, K., Doyle, J. C., Glover, K., et al. (1996). *Robust and optimal control*, volume 40. Prentice hall New Jersey.

RESPONSIBILITY NOTICE

The authors are the only responsibles for the material included in this paper.